Depletion effect during the synthesis of conductive graphene-based polymer composites

Khandaker Umaiya[†], Brenden Ferland,[‡] Douglas H. Adamson[†,‡,*]

[†]Department of Chemistry, University of Connecticut, Storrs, CT 06269, United States

[‡]Polymer Program, Institute of Materials Science, University of Connecticut, Storrs, CT 06269, United States

ABSTRACT: The synthesis of conductive graphene-based polymer composites remains a challenge due to suboptimal electrical conductivity compared to the theoretical potential of graphene. Here, we investigate the depletion effect during the polymerization of graphene-stabilized emulsions, leading to poly(high internal phase emulsions) (polyHIPEs) with a percolating graphene network. By monitoring electrical resistance and reaction temperature during the polymerization of styrene, methyl methacrylate, and tert-butyl acrylate systems, we provide evidence of the depletion effect, a phenomenon where high molecular weight polymer chains are excluded from confined graphene interfaces, enhancing graphene sheet-to-sheet contact and reducing electrical resistance. Systematic experiments reveal that polymerization parameters, including temperature, initiator presence, and crosslinking, govern conductivity transitions. These findings provide valuable insights into enhancing the design of graphene-based conductive composites for advanced applications.

Introduction

Graphene's delocalized π-electron network provides an electrical conductivity that rivals copper.[1–5] Harnessing that capability in bulk composites, however, remains elusive because the polymer matrix both interrupts percolation and imposes an interfacial contact resistance that can dominate the overall conduction path.[1,2] Typical graphene-polymer blends above their percolation threshold typically report conductivities below 10 $S \cdot m^{-1}$.[6,7] A compelling strategy to meet this challenge is to template the graphene into a segregated network that limits polymer intrusion.[8,9]

The segregated network approach is the strategy used by the solvent interface trapping method (SITM), in which pristine graphene spontaneously exfoliates at a water/oil interface, stabilizing a water-in-oil emulsion. The exfoliation of graphite in this system is spontaneous and driven by a lowering of the free energy of the system. Graphite has a surface tension greater than oil and less than water; when graphite is mixed with oil and water, it is trapped at the interface of two immiscible liquids; this difference in surface energy gives a positive spreading energy to the system that drives the exfoliation of graphite to graphene. If the system is shaken to create more interface, the extent of exfoliation increases [10–12]. This process forms a water-in-oil (W/O) emulsion with a percolating network of thin layers of graphene sheets.[11,13]

Using styrene (or another water insoluble monomer) as the oil phase, polymerized high internal phase emulsions (polyHIPEs) can be prepared. These materials are open-cell foams with the interior of the cells lined with a film of overlapping graphene sheets. However, we have observed that the resistance of the system dramatically decreases following the polymerization of the continuous phase. This is the opposite of what one might expect if, as generally thought, the decrease in electrical conductivity observed in graphene composites relative to pristine graphene is a result of the polymer matrix interrupting percolation and imposing interfacial contact resistance.

To understand what controls the electrical conductivity of these materials, we systematically investigated the mechanism of the graphene based polyHIPE preparation. The electrical conductivity of the system is a result of two mechanisms: electron hopping from sheet to sheet in the films of overlapping graphene sheets, and the electrical contact, or lack of contact, between the spheres that make up the polyHIPE composite. Since composites without sphere-to-sphere contact are closed cell, our open cell morphology suggests that a lack of sphere-to-sphere contact is not the factor controlling conductivity. Therefore, we concentrated on the film of overlapping graphene sheets that make up the segregated network. To do this, we monitored how the electrical resistance of the graphene stabilized emulsions progressed during the polymerization of the continuous phase. Varying system parameters during the polymerization allowed us to test various mechanistic hypothesis describing the evolution of the final measured electrical conductivity.

Results and Discussion

PolyHIPE Morphology

The composites examined in this study are produced by polymerizing the continuous phase of a graphene-stabilized water-in-oil emulsion. The graphene was produced by exfoliating graphite at the oil/water interface during the shaking of a water, monomer (oil), and graphite mixture. The graphene spreads at the interface, lowering the free energy of the system much like a small molecule surfactant[14]. These emulsions are placed in an oven and heated to initiate polymerization via a thermal initiator dissolved in the oil phase. The result is an open-cell foam material with a percolating graphene network that is electrically conductive[9,15]. Details of the approach are included in the Experimental Section.

Figure 1 shows SEM images of the graphene-stabilized polyHIPE open-cell foam with the cells lined with a film of overlapping graphene sheets. The holes, or windows occurred where there was sphere-to-sphere contact. In those regions, there was no polymer; only a thin film of overlapping graphene. This film was easily broken, giving rise to windows between the spheres that allowed for the removal of the dispersed water phase.

Additionally, some unexfoliated graphite can be seen, as exfoliation stops once the oil/water interface is covered by the graphene film. The exfoliation of graphite and the spreading of graphene occur because of the high-energy interface between oil and water. Once the spreading graphene has stabilized this interface, there is no longer a driving force for exfoliation, and thus, excess graphite remains.

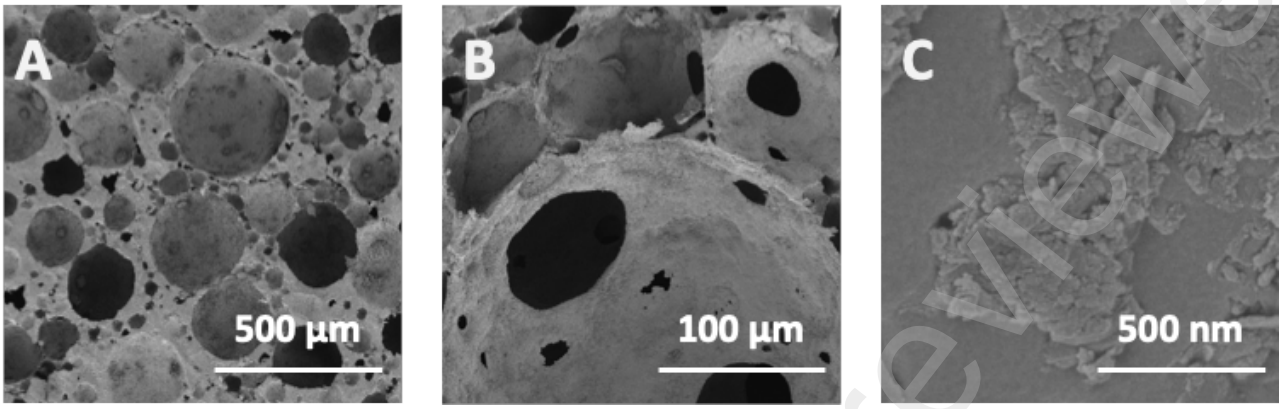

Figure 1. SEM images of graphene stabilized polyHIPE. **A)** Image showing the open cell morphology of the polyHIPE. **B)** Higher magnification image of windows between spheres. **C)** Graphene at the surface of the polyHIPE cells. Most the graphene is embedded in the polymer.

Effect of Polymerization on Conductivity

A common explanation for electrical resistance in segregated networks is that polymer forms between the graphene sheets, serving as an electrical insulator, disrupting percolation, and creating interfacial contact resistance. If that were the case in our system, then the emulsion might be expected to be more electrically conductive prior to polymerization of the continuous oil phase. To test this hypothesis, we placed electrodes in the emulsion and measured the resistance as a function of time during polymerization of the oil phase.

Figure 2A shows the change in electrical resistance as the polymerization of the continuous phase progressed. The initial resistance was 5.19 kΩ, and after 45 minutes in an oven set to 65 °C, the resistance decreased to 3.79 kΩ, which we attributed to the emulsion draining, increasing the contact area between the graphene-coated spheres. In any emulsion with differences in the densities of the two phases, the system will drain, and the dispersed phase will pack more closely as the continuous phase either drains or rises from between the droplets.

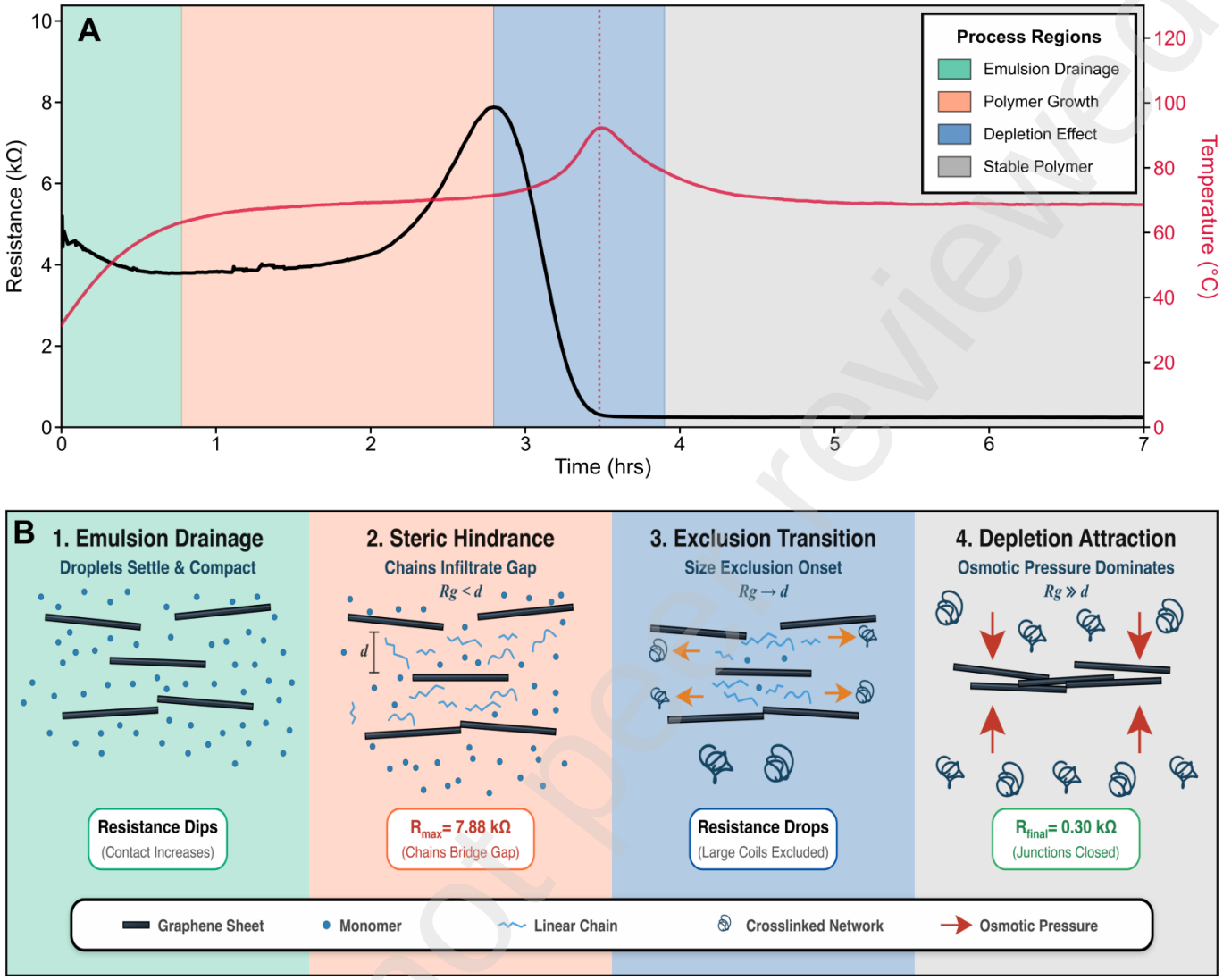

Figure 2. Electrical resistance evolution during polymerization and proposed depletion mechanism. (A) With crosslinker showing four process regions (shaded): emulsion drainage (teal), polymer growth (orange), depletion effect (blue), and stable polymer (gray). Red dotted line marks peak exotherm. **(B)** Schematic illustration of depletion mechanism across four stages: (1) Emulsion drainage with dispersed monomers between graphene sheets; (2) Steric hindrance as linear polymer chains (Rg < d) infiltrate gap between sheets; (3) Exclusion transition where growing crosslinked networks (Rg → d) begin size exclusion; (4) Depletion attraction where large crosslinked polymers (Rg ≫ d) are excluded from confined regions, generating osmotic pressure that drives sheet-to-sheet contact. Rg is the polymer radius of gyration and d is the gap width between graphene sheets. Legend shows graphene sheets (black bars), monomers (blue dots), linear chains (blue wavy lines), crosslinked networks (gray coils), and osmotic pressure (red arrows).

After the emulsion drained, the resistance then began to increase. At just over two hours in the oven, the resistance reached a maximum of 7.88 kΩ. This increase in resistance corresponded to the onset of polymerization as the reaction warmed to the oven temperature and polymers grew between the graphene sheets. However, the maximum in resistance occurred before the maximum reaction temperature was reached. Since the polymerization of styrene is exothermic, the temperature of the reaction increased above the oven temperature as the reaction accelerated.

After about 3 hours, the reaction temperature increased to 92 °C before cooling to the oven's temperature, an indication that the polymerization was done. Unexpectedly, the peak in the temperature of polymerization directly correlated with a dramatic decrease in resistance, with the resistance of the system dropping precipitously, reaching 0.30 kΩ at nearly the same time as the system reached its maximum temperature. It then remained at that resistance as the reaction cooled to the oven temperature.

These results suggest that after the electrical resistance reduction due to draining, the resistance began to increase as the system's temperature increased and polymerization began. This supported the idea that the presence of polymers in our segregated conductive network created an insulating layer between the graphene sheets, interrupting electrical percolation. However, as the polymerization proceeded and accelerated, the unexpected steep decrease in resistance suggests an additional mechanism.

Proposed Mechanism

The electrical resistance of a percolated graphene network is dominated by a small number of sheet–sheet junctions where electrons tunnel across nanometer scale gaps. Because tunneling decays exponentially with gap width, any polymer in the junction raises the barrier and increases resistance, as observed after the during the early stages of polymer growth stage in **Figure 2A**. Alternatively, removing polymer from the gap would result in a sharp, decrease in resistance.[16–18]

Initially, the graphene sheets were separated by monomer molecules. As the reaction warmed and the thermal initiator began to generate radicals, a mixture of low-molecular-weight chains and monomer occupied the regions between the sheets, creating an insulating layer. As the polymerization progressed, the concentration of monomer decreased, increasing the likelihood of growing radical chains reacting with unreacted double bonds in other polymer chains that were incorporated by the occasional addition divinyl benzene monomers. Growing chains reacting with other chains quickly increased the size of the chains,[19] and once the coil size was greater than the slit width, the chains were excluded from the gap and the resulting osmotic-pressure imbalance generated a depletion attraction between the facing sheets. In the plate–plate geometry relevant here, theory predicts polymer expulsion from the slit as soon as the coil's size exceeds the accessible gap,[20] lowering the tunneling barrier and resistance.

Our proposed depletion mechanism, shown schematically in **Figure 2B**, is typically observed in colloidal particle systems when non-adsorbing solutes such as polymers are added to a dispersion of larger colloidal particles. These polymers create an osmotic pressure imbalance that leads to an effective attraction between the larger colloidal particles[24–26]. This occurs because the polymers with R_g values greater than the distance between two colloids are excluded from the space between the approaching particles, reducing the local osmotic pressure. As a result, the surrounding fluid exerts a net force that pushes the large particles together, leading to aggregation[25,27,28].

The conversion of monomers to polymers also leads to an increase in viscosity. At some point, the graphene sheets cannot rearrange. Even without the use of crosslinkers, the increase in viscosity leads to auto acceleration, or the Trommsdorff effect,[19] where termination reactions are so slow that growing chains don't terminate by coupling and react with other polymers, leading to gelation. In our formulations, the added crosslinker accelerates the effective growth of coil size so the depletion threshold is reached before the system gels and immobilizes the graphene sheets.

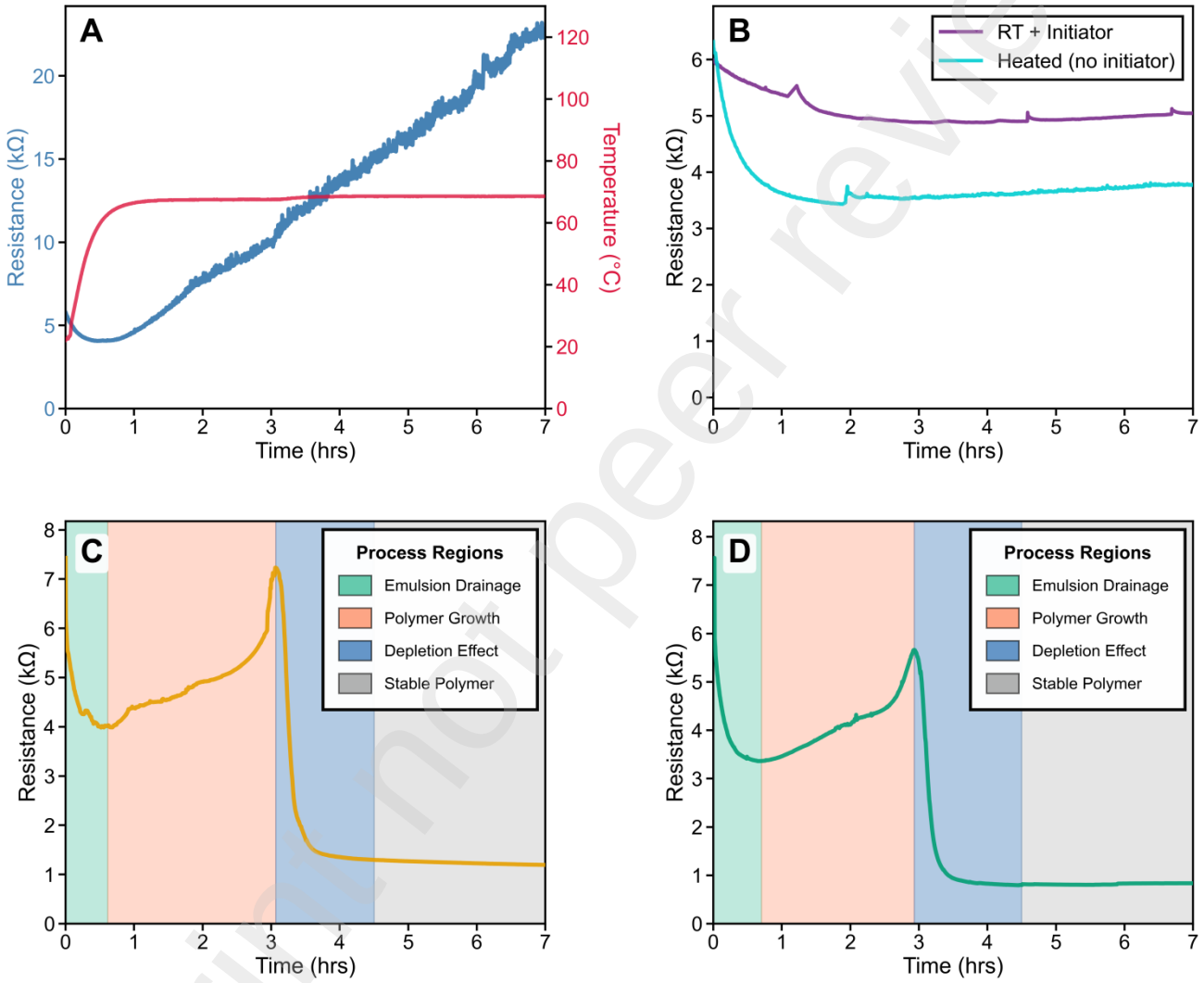

Figure 3. Electrical resistance evolution during emulsion polymerization of graphene-stabilized monomer emulsions. **(A)** Resistance (left axis, steel blue) and temperature (right axis, red) measured during polymerization of polystyrene WITHOUT DVB crosslinker. **(B)** Control experiments: styrene emulsion at room temperature with initiator (purple) and styrene emulsion heated to 65°C without initiator (cyan). **(C)** Resistance measured during polymerization of methyl methacrylate (MMA) with DVB crosslinker (orange line). Shaded regions indicate MMA-specific process phases: emulsion drainage (teal), polymer growth (orange), depletion effect (blue), and stable polymer (gray). **(D)** Resistance measured during polymerization of tert-butyl acrylate (PtBA) with DVB crosslinker (green line). Shaded regions indicate PtBA-specific process phases using the same color scheme as panel C.

Testing the hypothesis

To test our proposed mechanism, we repeated our previous studies, this time without using the DVB crosslinker. Our mechanism depends on the rapid increase of polymer chain size prior to the exotherm

normally associated with the Trommsdorff effect. In the free radical polymerization of monomers containing only one vinyl group, the MW of the polymers produced stays fairly constant during most of the reaction. Unless a crosslinker is added, there is normally no spike in MW, or polymer size, during the polymerization. This suggests that without crosslinker, the number of polymer chains between the graphene sheets would increase, but their size would not. Since the polymer coil size is the critical driving force behind the depletion effect, simply increasing the number of chains separating the sheets would result in a steady increase in the network resistivity. The change in resistance as a function of time in a system without crosslinker is shown in **Figure 3A**.

As with the crosslinked systems, we observed an initial decrease in the resistance, followed by an increase. Unlike the systems with crosslinker, however, the resistance did not decrease with further conversion; instead, it continued to increase during the reaction. This dramatic difference in the system's behavior highlights the necessity of the crosslinker, and a rapid increase in MW. We also observed a very different temperature profile when not using DVB. There was no maximum observed, just a steady temperature that matched the temperature of the oven. We expect that the difference was a result of the lower viscosity of the system in the absence of crosslinking.

To test that simple drainage was the cause of the initial resistance increase rather than a temperature change decreasing the interfacial tension that pins the graphene sheets, we carried out two control reactions to be sure our resistance observations were not simply a result of system aging. First, we prepared an emulsion with the typical component and monitored the resistance without placing it in an oven. The result is shown in **Figure 3B**. We observed an initial decrease in resistance, consistent with the draining observed in **Figure 2A**. Unlike the results shown in **Figure 2A**, however, there was no resistance maximum followed by a sharp resistance drop. Instead, we observed a gradual leveling of the resistance value with increasing time.

Another control, also shown in **Figure 3B**, observed an emulsion system prepared without an initiator, but heated in an oven at 65 °C. Again, there was an initial drop in resistance, but no maxima or resistance drop. Just the resistance is gradually leveling off. These results suggest that the initial drop in resistance was indeed a result of the emulsion's dynamics, but that the subsequent observations were due to the polymerization reaction.

Our original hypothesis to explain this decrease in resistance was that polymer bridging brings the sheets closer together. Bridging flocculation is well known in colloid science,[22] where polymer chains absorb on separate particles and draw them together. The known π-π interaction of polystyrene with graphene[23] made this mechanism attractive and testable by investigating monomers that did not have π-π interactions with graphene. We did this by repeating the study shown in **Figure 2A** with monomers

lacking the π-π interactions with graphene. Shown in **Figure 3C** is the result of using methyl methacrylate rather than styrene as the monomer (oil phase).

Although methyl methacrylate is more hydrophilic than styrene, both monomers form graphene-stabilized water-in-oil emulsions, and the plots of resistance as a function of time were similar. As seen in **Figure 3D**, the same is true for *t*-butyl-acrylate. This result suggests that the reduction of resistance is not a function of bridging flocculation. Additionally, this mechanism would result in polymer chains remaining between the sheets, making the observed sharp decrease in resistance unlikely.

Shrinkage during polymerization may play a role, however. Polymerization of monomers leads to a reduction in volume, and significant shrinkage is known for both styrene and acrylates, with methyl methacrylate shrinking ~21% and styrene shrinking ~14% when polymerized.[21] We observed that although methyl methacrylate is known to shrink more than styrene, the reduction of resistance in the styrene system was greater than in the methyl methacrylate system, evidence that although shrinkage may play a role, it is not driving force behind the decrease in resistance. Additionally, shrinkage alone would mean that polymer remained between the graphene sheets.

Conclusion

This study highlights the pivotal role of the depletion effect in modulating the electrical conductivity of graphene-based polymer composites during the polymerization process. By systematically varying polymerization conditions, including monomer type, temperature, and crosslinker presence, we demonstrated the interplay between polymer chain exclusion and graphene sheet-to-sheet contact. The exclusion of high molecular weight polymers from graphene interfaces increases system entropy, facilitating closer graphene interactions and reducing resistance.

The findings elucidate critical mechanisms influencing conductivity in graphene composites and provide a framework for optimizing polymerization protocols to achieve superior electrical properties. Future work could explore alternative stabilizers, dynamic monitoring of the depletion zone, and the influence of emulsion morphology on percolation thresholds. These insights are poised to advance the design of high-performance materials for applications in energy storage, sensors, and electronics.

Experimental

Materials

Styrene (Sigma Aldrich, Reagent Plus, 99%), methyl methacrylate (Acros Organics, 99%,), tert-butyl acrylate (Acros Organics, 99%), 2,2′-azobis(2-methylpropionitrile) (Sigma Aldrich, 98%), divinyl benzene (Sigma Aldrich, technical grade, 80%), graphite (Asbury Carbon, Nano 24, synthetic 1μm flake size) were used as received. All samples are made in 30 ml vials.

Formation of graphene-stabilized monomer emulsion

A 30 ml vial was charged with 14 ml of deionized water, 6ml of monomer: styrene or methyl methacrylate (MMA) or tert-butyl acrylate (t-BA), 1.4 ml of the crosslinker divinyl benzene (DVB), 0.467 g of graphite nano 24 (GN24), and 0.018g of the initiator 2,2′-azobis(2-methylpropionitrile) (AIBN). The

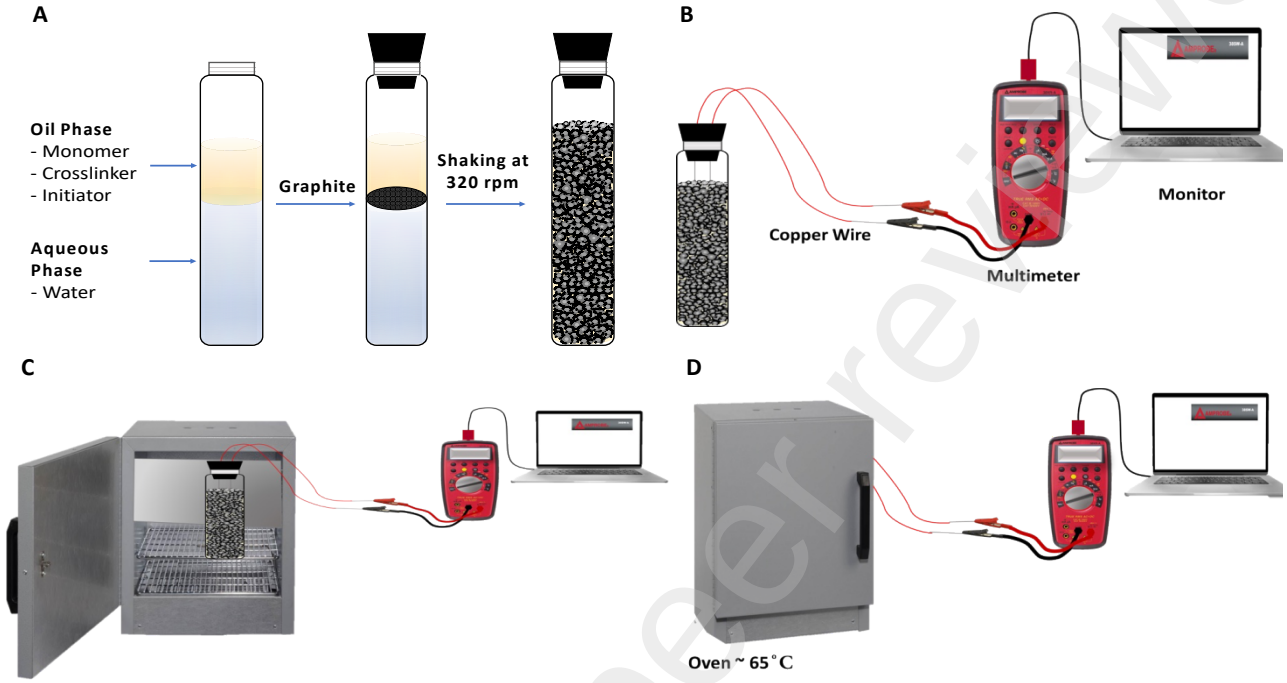

Scheme 1. **(A)** The schematic diagram of the synthesis process of polystyrene-graphene composite. **(B)-(D)** The representation of the resistance measurement.

vials were then shaken for 2 minutes using a bubble tea shaker (Happybuy Milk Tea shaker, 320 rpm) to exfoliate the graphite **(Scheme 1-A)**. Control samples were made without DVB and AIBN, and additionally, some samples were monitored at room temperature.

Resistance study during the polymerization

Copper wires (28 AWG) were inserted into the vial containing the solution mixture through a rubber stopper, keeping them 10mm apart in the emulsion. The vials were placed into a Blue M, Stabil-Therm convection oven at ~70 °C for 24 hours. Resistance was measured using an Amprobe 38XR-A digital multimeter with Amprobe 38SW-A RS-232 software for data logging (Scheme 1B-D). Resistance data were recorded at 15-second intervals for 7 hours during polymerization.

Temperature Study during the polymerization

To measure the temperature of the system, a K-type thermocouple probe was inserted into the vial before placing it in the oven, and the temperature change was recorded at 15-second intervals for 7 hours using Omega OM-74 thermocouple logger and OM-70 series interface program software.

Morphological analysis

For morphological analysis, a scanning electron microscope (FEI Nova NanoSEM 450) was used. Polymerized solid composites were cut into 1mm pieces, attached to an aluminum stub using carbon tape, coated with Au/Pd in a sputter coater, and imaged using SEM at 50, 250, and 50,000 magnifications under high vacuum.

References:

(1) Stankovich, S.; Dikin, D. A.; Dommett, G. H. B.; Kohlhaas, K. M.; Zimney, E. J.; Stach, E. A.; Piner, R. D.; Nguyen, S. T.; Ruoff, R. S. Graphene-Based Composite Materials. *Nature* **2006**, *442* (7100), 282–286. https://doi.org/10.1038/nature04969.

(2) Araby, S.; Meng, Q.; Zhang, L.; Mu, M.; Wan, C.; Gorgolis, G.; Galiotis, C. Electrical Percolation in Graphene – Polymer Composites Electrical Percolation in Graphene – Polymer Composites. **2018**.

(3) Marsden, A. J.; Papageorgiou, D. G.; Vallés, C.; Liscio, A.; Palermo, V.; Bissett, M. A.; Young, R. J.; Kinloch, I. A. Electrical Percolation in Graphene-Polymer Composites. *2D Materials* **2018**, *5* (3). https://doi.org/10.1088/2053-1583/aac055.

(4) Alam, A.; Meng, Q.; Shi, G.; Arabi, S.; Ma, J.; Zhao, N.; Kuan, H. C. Electrically Conductive, Mechanically Robust, pH-Sensitive Graphene/Polymer Composite Hydrogels. *Composites Science and Technology* **2016**, *127*, 119–126. https://doi.org/10.1016/j.compscitech.2016.02.024.

(5) Fang, X.-Y.; Yu, X.-X.; Zheng, H.-M.; Jin, H.-B.; Wang, L.; Cao, M.-S. Temperature- and Thickness-Dependent Electrical Conductivity of Few-Layer Graphene and Graphene Nanosheets. *Physics Letters A* **2015**, *379* (37), 2245–2251. https://doi.org/10.1016/j.physleta.2015.06.063.

(6) Sun, X.; Huang, C.; Wang, L.; Liang, L.; Cheng, Y.; Fei, W.; Li, Y. Recent Progress in Graphene/Polymer Nanocomposites. *Advanced Materials* **2021**, *33* (6), 2001105. https://doi.org/10.1002/adma.202001105.

(7) Pang, H.; Chen, T.; Zhang, G.; Zeng, B.; Li, Z.-M. An Electrically Conducting Polymer/Graphene Composite with a Very Low Percolation Threshold. *Materials Letters* **2010**, *64* (20), 2226–2229. https://doi.org/10.1016/j.matlet.2010.07.001.

(8) Zhang, T.; Sanguramath, R. A.; Israel, S.; Silverstein, M. S. Emulsion Templating: Porous Polymers and Beyond. *Macromolecules* **2019**, *52* (15), 5445–5479. https://doi.org/10.1021/acs.macromol.8b02576.

(9) Bento, J. L.; Brown, E.; Woltornist, S. J.; Adamson, D. H. Thermal and Electrical Properties of Nanocomposites Based on Self-Assembled Pristine Graphene. *Advanced Functional Materials* **2017**, *27* (1). https://doi.org/10.1002/adfm.201604277.

(10) Coleman, J. Liquid-Phase Exfoliation of Nanotubes and Graphene. *Advanced Functional Materials* **2009**, *19*, 3680–3695. https://doi.org/10.1002/adfm.200901640.

(11) Coleman, J. N.; Lotya, M.; O'Neill, A.; Bergin, S. D.; King, P. J.; Khan, U.; Young, K.; Gaucher, A.; De, S.; Smith, R. J.; Shvets, I. V.; Arora, S. K.; Stanton, G.; Kim, H.-Y.; Lee, K.; Kim, G. T.; Duesberg, G. S.; Hallam, T.; Boland, J. J.; Wang, J. J.; Donegan, J. F.; Grunlan, J. C.; Moriarty, G.; Shmeliov, A.; Nicholls, R. J.; Perkins, J. M.; Grieveson, E. M.; Theuwissen, K.; McComb, D. W.; Nellist, P. D.; Nicolosi, V. Two-Dimensional Nanosheets Produced by Liquid Exfoliation of Layered Materials. *Science* **2011**, *331* (6017), 568–571. https://doi.org/10.1126/science.1194975.

(12) Wang, S.; Zhang, Y.; Abidi, N.; Cabrales, L. Wettability and Surface Free Energy of Graphene Films. *Langmuir : the ACS journal of surfaces and colloids* **2009**, *25*, 11078–11081. https://doi.org/10.1021/la901402f.

(13) Poon, W. Colloids as Big Atoms. *Science* **2004**, *304* (5672), 830–831. https://doi.org/10.1126/science.1097964.

(14) Woltornist, S. J.; Oyer, A. J.; Carrillo, J. M. Y.; Dobrynin, A. V.; Adamson, D. H. Conductive Thin Films of Pristine Graphene by Solvent Interface Trapping. *ACS Nano* **2013**, *7* (8), 7062–7066. https://doi.org/10.1021/nn402371c.

(15) Brown, E. E. B.; Woltornist, S. J.; Adamson, D. H. PolyHIPE Foams from Pristine Graphene: Strong, Porous, and Electrically Conductive Materials Templated by a 2D Surfactant. *Journal of Colloid and Interface Science* **2020**, *580*, 700–708. https://doi.org/10.1016/j.jcis.2020.07.026.

(16) Hashemi, R.; Weng, G. J. A Theoretical Treatment of Graphene Nanocomposites with Percolation Threshold, Tunneling-Assisted Conductivity and Microcapacitor Effect in AC and DC Electrical Settings. *Carbon* **2016**, *96*, 474–490. https://doi.org/10.1016/j.carbon.2015.09.103.

(17) Hicks, J.; Behnam, A.; Ural, A. A Computational Study of Tunneling-Percolation Electrical Transport in Graphene-Based Nanocomposites. *Applied Physics Letters* **2009**, *95* (21), 213103. https://doi.org/10.1063/1.3267079.

(18) Oskouyi, A.; Sundararaj, U.; Mertiny, P. Tunneling Conductivity and Piezoresistivity of Composites Containing Randomly Dispersed Conductive Nano-Platelets. *Materials* **2014**, *7* (4), 2501–2521. https://doi.org/10.3390/ma7042501.

(19) O'Shaughnessy, B.; Yu, J. Autoacceleration in Free Radical Polymerization. *Phys. Rev. Lett.* **1994**, *73* (12), 1723–1726. https://doi.org/10.1103/PhysRevLett.73.1723.

(20) Schlesener, F.; Hanke, A.; Klimpel, R.; Dietrich, S. Polymer Depletion Interaction between Two Parallel Repulsive Walls. *Phys. Rev. E* **2001**, *63* (4), 041803. https://doi.org/10.1103/PhysRevE.63.041803.

(21) Nichols, F. S.; Flowers, R. G. Prediction of Shrinkage in Addition Polymerizations. *Ind. Eng. Chem.* **1950**, *42* (2), 292–295. https://doi.org/10.1021/ie50482a024.

(22) Swenson, J.; Smalley, M. V.; Hatharasinghe, H. L. M. Mechanism and Strength of Polymer Bridging Flocculation. *Phys. Rev. Lett.* **1998**, *81* (26), 5840–5843. https://doi.org/10.1103/PhysRevLett.81.5840.

(23) Luo, J.-T.; Zha, H.; Tian, H.-K.; Zuo, B. Physical Adsorption and Glass Transition of Thin Polystyrene Films at a Graphene Interface. *Chin J Polym Sci* **2025**, *43* (7), 1163–1169. https://doi.org/10.1007/s10118-024-3241-2.

(24) Kim, J. S.; Szleifer, I. Depletion Effect on Polymers Induced by Small Depleting Spheres. *J. Phys. Chem. C* **2010**, *114* (48), 20864–20869. https://doi.org/10.1021/jp107598m.

(25) Egorov, S. A. Depletion Interactions between Nanoparticles: The Effect of the Polymeric Depletant Stiffness. *Polymers* **2022**, *14* (24), 5398. https://doi.org/10.3390/polym14245398.
(26) Yodh, A. G.; Lin, K. H.; Crocker, J. C.; Dinsmore, A. D.; Verma, R.; Kaplan, P. D. Entropically Driven Self-Assembly and Interaction in Suspension. *Philosophical Transactions of the Royal Society A: Mathematical, Physical and Engineering Sciences* **2001**, *359* (1782), 921–937. https://doi.org/10.1098/rsta.2000.0810.
(27) Shim, Y. H.; Lee, K. E.; Shin, T. J.; Kim, S. O.; Kim, S. Y. Tailored Colloidal Stability and Rheological Properties of Graphene Oxide Liquid Crystals with Polymer-Induced Depletion Attractions. *ACS Nano* **2018**, *12* (11), 11399–11406. https://doi.org/10.1021/acsnano.8b06320.
(28) Ji, S.; Walz, J. Y. Synergistic Effects of Nanoparticles and Polymers on Depletion and Structural Interactions. *Langmuir* **2013**, *29* (49), 15159–15167. https://doi.org/10.1021/la403473g.